

Memristor-Based MobileNetV3 Circuit Design for Image Classification

Jiale Li

*School of Computer Science
The University of Auckland
Auckland, New Zealand
jli990@aucklanduni.ac.nz*

Yulin Fu

*School of Computer Science
The University of Auckland
Auckland, New Zealand
yxue732@aucklanduni.ac.nz*

Dongwei Yan

*School of Computer Science
The University of Auckland
Auckland, New Zealand
dyan232@aucklanduni.ac.nz*

Sean Longyu Ma

*School of Computer Science
The University of Auckland
Auckland, New Zealand
sean.ma@auckland.ac.nz*

Chiu-Wing Sham

*School of Computer Science
The University of Auckland
Auckland, New Zealand
b.sham@auckland.ac.nz*

Chong Fu

*School of Computer Science
and Engineering
Northeastern University
Shenyang, China
fuchong@mail.neu.edu.cn*

Abstract—The increasing computational demands of deep learning models pose significant challenges for edge devices. To address this, we propose a memristor-based circuit design for MobileNetV3, specifically for image classification tasks. Our design leverages the low power consumption and high integration density of memristors, making it suitable for edge computing. The architecture includes optimized memristive convolutional modules, batch normalization modules, activation function modules, global average pooling modules, and fully connected modules. Experimental results on the CIFAR-10 dataset show that our memristor-based MobileNetV3 achieves over 90% accuracy while significantly reducing inference time and energy consumption compared to traditional implementations. This work demonstrates the potential of memristor-based designs for efficient deployment of deep learning models in resource-constrained environments.

Index Terms—memristor, machine learning, MobileNetV3, circuit design

I. INTRODUCTION

The advancement of deep neural networks (DNNs) has led to significant improvements in complex tasks such as image classification. However, the increasing computational demands of these models pose substantial challenges, particularly for edge devices with limited resources [1]. MobileNetV3, designed for efficient deployment on edge devices, offers a promising solution by reducing computational load while maintaining high accuracy [2]. Nevertheless, even lightweight networks like MobileNetV3, while significantly reducing parameter count compared to larger models, still often contain millions of parameters, making their deployment on resource-constrained edge devices challenging. To address these limitations, we propose a novel memristor-based circuit design for MobileNetV3, specifically tailored for image classification tasks on edge devices. This approach leverages neuromorphic computing principles to achieve hardware-software synergy, maximizing the advantages of low power consumption and rapid inference speed.

Our design utilizes memristor crossbars to perform vector-matrix multiplications (VMMs) efficiently in the analog domain. The circuit architecture comprises several key modules: memristor-based convolution module, memristor-based batch normalization module, activation function module, memristor-based global average pooling module, and memristor-based fully connected module. It also includes addition modules for residual connections [3] and multiplication modules in the attention modules. In this computing paradigm, multiplication is executed using Ohm's Law, and summation is achieved through Kirchhoff's Current Law [4]. Trained weights are stored as memristor conductance values, eliminating the need for data movement between computing and memory units and thereby reducing energy consumption [5]. In summary, this paper makes the following main contributions:

- We propose a novel memristor-based computing paradigm and hardware design for MobileNetV3, achieving over 90% accuracy on CIFAR-10 with significant advantages in resource utilization, computation time, and power efficiency.
- We design four memristor-based modular circuits for layer normalization, hard sigmoid, hard swish, and convolution for the first time. Our simplified design reduces the number of operational amplifiers (op-amps) by 50% in convolutional and fully connected layers compared to conventional methods.

II. CIRCUIT DESIGN

A. Network Architecture

The MobileNetV3 architecture consists of four main memristor-based neural network units, as illustrated in Figure 1. Our computing paradigm follows the neural network layers described in [6]. The network begins with an input layer for image preprocessing, incorporating convolution, normalization, and hard swish activation. This is followed by a body

layer containing multiple bottleneck blocks with lightweight attention modules based on squeeze and excitation. A final convolutional layer, comprising convolution, normalization, and hard swish activation, precedes the classification layer. This final layer features global average pooling, two fully connected sub-layers, and a hard swish activation, which are crucial for achieving accurate image classification.

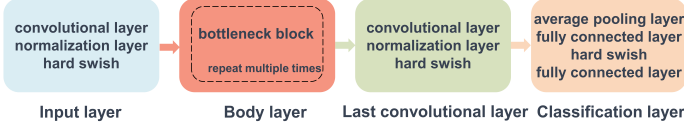


Fig. 1. Flowchart of the network architecture based on MobileNetV3.

B. Memristor-Based Convolution Module

In this computing paradigm, there are three types of convolution operations: regular convolution, depthwise convolution, and pointwise convolution. The differences among these convolution operations are as follows: In regular convolution, memristors are placed at specific locations on a crossbar to perform the sliding window operation, and their output currents are interconnected for a summation function. In contrast, depthwise convolution lacks this summation operation compared to regular convolution [7]. Pointwise convolution is similar to one-channel regular convolution [8]. Based on the analysis above, we will focus on regular convolution as a case study to present the implementation details of the memristor crossbar.

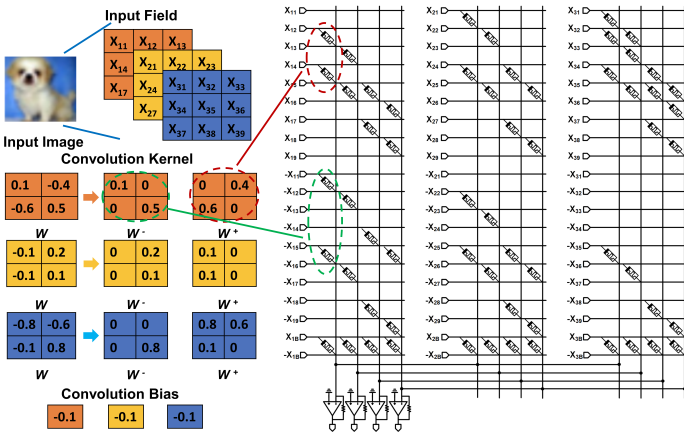


Fig. 2. Circuit schematic of memristor crossbars for a convolution operation.

To perform the convolution operation between the memristor-based convolutional kernel and the input matrix, it is necessary to split the original weight matrix into positive and negative matrices firstly since the resistance of a single memristor is positive. As shown in Figure 2, contrary to the conventional approach in most research papers [9]–[11], we designate the matrix with positive weights as the negative weight matrix, mapping the negative weight matrix to that part of the memristor crossbar consisting of the inverting

inputs, while the matrix with negative weights is labelled as the positive weight matrix, corresponding to the original inputs of the memristor crossbar. The output current has the opposite polarity to the actual result. After passing through the trans-impedance amplifier (TIA), it is converted into a voltage with the same polarity as the actual result, due to the TIA's inverting nature. Compared to aforementioned solutions, the most significant advantage of this method is that it reduces the number of op-amps at each output port. Given that the power consumption of op-amps is at the mW level while that of memristors is at the μ W level [12], this approach is indeed meaningful.

Secondly, the number of rows (O_r) and the number of columns (O_c) in the output matrix are determined by the formulas:

$$O_{r|c} = \left(\frac{W_{r|c} - F_{r|c} + 2P}{S} + 1 \right) \quad (1)$$

where $O_{r|c}$, $W_{r|c}$, and $F_{r|c}$ represent the number of rows or columns in the output matrix, input matrix, and convolutional kernel matrix, respectively. P and S stand for padding and stride, respectively.

Thirdly, the padded input matrix is utilized as the new input matrix and is unfolded row-wise to serve as the positive input. Subsequently, the negation of this new input matrix is employed as the negative input. The starting position of each output memristor in the positive and negative input regions is determined by the following equations:

$$P_{Pi} = \left(\lfloor \frac{i}{O_c} \rfloor * W_c + i \bmod O_c \right) * S, i \in \mathbb{N} \quad (2)$$

$$P_{Ni} = \left(\lfloor \frac{i}{O_c} \rfloor * W_c + i \bmod O_c \right) * S + W_r * W_c, i \in \mathbb{N} \quad (3)$$

where i is the output index, and P_{Pi} , P_{Ni} represent the starting position of O'_i in the positive and negative input regions respectively. In other words, this formula indicates that (O'_i, P_{Pi}) are the coordinates for placing the first memristor in each column. Similarly, (O'_i, P_{Ni}) are the coordinates for placing the first memristor in the negative input regions of each column.

Fourthly, the convolutional kernel is unfolded into a single-row matrix. Starting from (O'_i, P_{Pi}) , sequentially assign F_c memristors with weights to the memristor crossbars, and repeat the process with an interval of $(W_c - F_c + 2P)$. It is worth noting that memristors with a weight of zero do not appear in the memristor crossbar to reduce the number of memristors, as their contribution to the output is zero. Then, starting from (O'_i, P_{Ni}) , assign memristors in the negative input area according to the above rules. The two bias voltages, as the last inputs, combined with the memristors, form the bias for the convolution operation.

Finally, the convolution operation formula in memristor crossbars is expressed by the following equation:

$$V_j = - \sum_{i=0}^{2N+1} \frac{V_i}{R_{i,j}} * R_f, i \in \mathbb{N}, j \in \mathbb{N} \quad (4)$$

where V_i is the $(i)^{th}$ input voltage in the memristor crossbar. $R_{i,j}$ represents the resistance of the memristor at the (i, j) position, if it exists. R_f stands for the feedback resistance in the TIA. The negative sign in the formula is determined by the properties of the TIA. V_j is the $(j)^{th}$ output voltage, which corresponds to the $(j)^{th}$ element of the one-dimensional matrix obtained by flattening the convolution result matrix.

C. Memristor-Based Batch Normalization Module

The batch normalization module is extensively utilized in the MobileNetV3 network architecture to achieve both excellent accuracy and efficiency. The calculation method is as follows:

$$y = \frac{x - E[x]}{\sqrt{Var[x] + \epsilon}} * \gamma + \beta \quad (5)$$

where x represents the original feature value, $E[x]$ is the mean, and $Var[x]$ is the variance, with epsilon serving as a small constant to prevent division by zero. γ and β are the learnable scaling and shifting parameters, respectively. y is the output of the batch normalization module. Owing to the applicability of memristor crossbars for multiplication and addition computations, the batch normalization formula is segmented into three components: subtraction, multiplication, and addition operations. The converted formulas are as follows:

$$y = (x - E[x]) * \left| \frac{\gamma}{\sqrt{Var[x] + \epsilon}} \right| + \beta, \gamma \geq 0 \quad (6)$$

$$y = (E[x] - x) * \left| \frac{\gamma}{\sqrt{Var[x] + \epsilon}} \right| + \beta, \gamma < 0 \quad (7)$$

In this circuit design, memristors and TIAs are employed to execute the batch normalization operation. Specifically, the subtraction part comprises four input ports and two memristors, with the output converted to voltage via TIA for subsequent multiplication operation. Addition is achieved like biasing in convolution operations. To minimize the use of op-amps in the design of the batch normalization module, a set of specific rules is followed. V_b is set to a constant value of one. As shown in Figure 3(a), when the input value γ is non-negative, the resistance values of the first set of memristors are sequentially set to (1, 0, 0, 1), facilitating the subtraction operation $(x - E[x])$. The resistance values of the second set of memristors depend on the sign of β . For positive β , the values are set to $(\left| \frac{\gamma}{\sqrt{Var[x] + \epsilon}} \right|, 0, \frac{1}{\beta})$; for negative β , they are set to $(\left| \frac{\gamma}{\sqrt{Var[x] + \epsilon}} \right|, \frac{1}{\beta}, 0)$. As shown in Figure 3(b), in cases where γ is negative, the first set of memristors is set to (0, 1, 1, 0) to achieve the subtraction operation $(E[x] - x)$, while the second set follows the same resistance value assignment as in the non-negative case. This approach effectively reduces the need for op-amps and enhances the overall efficiency of the batch normalization module.

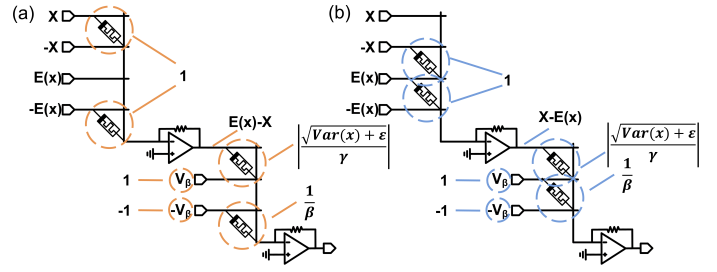


Fig. 3. Circuit schematic of memristor crossbars for a batch normalization operation. (a) $\gamma \geq 0, \beta > 0$ (b) $\gamma < 0, \beta < 0$.

D. Activation Function Module

In MobileNetV3, three types of activation functions are utilized: ReLU, hard sigmoid, and hard swish. The implementation of ReLU in this paper is based on the paper published before [13]. Furthermore, we designed the hard sigmoid and hard swish activation function circuits, as shown in Figures 4(a) and 4(b). In the circuit implementation, op-amps are utilized to carry out addition and division operations. The limiter, constructed from a diode and a power source, serves the crucial role of executing the maximization function. Compared with the hard sigmoid activation function module, the hard swish module has an additional multiplication operation consisting of a multiplier. According to the simulation results shown in Figures 4(c) and 4(d), it is evident that this module achieves the functional objectives consistent with those of the software design.

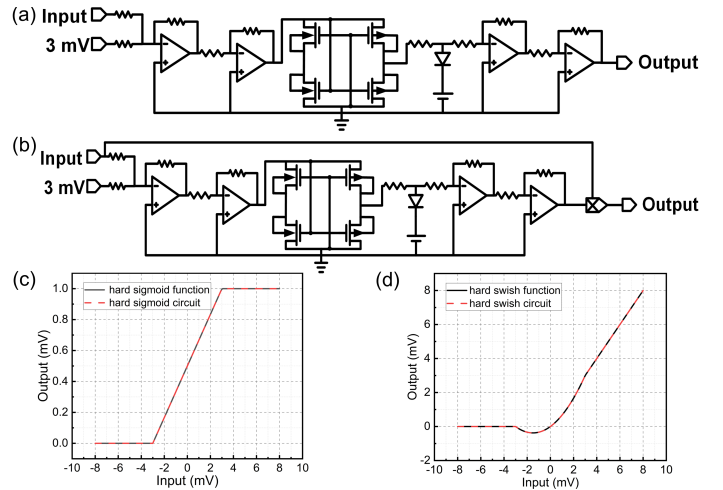


Fig. 4. Circuit schematic of an activation function operation. (a) hard sigmoid, (b) hard swish, and simulation result (c) hard sigmoid, (d) hard swish.

E. Memristor-Based Global Average Pooling Module

In MobileNetV3, the global average pooling is positioned at the terminus of the network, where it transforms the deep convolutional feature maps into a one-dimensional feature vector. This resultant feature vector is subsequently utilized for classification tasks. Figure 5(a) illustrates the process of

performing global average pooling computations in the memristor crossbars. The inverse of the input matrix is unfolded into a one-dimensional vector and applied as voltage to the input terminals of the memristor crossbar. The weight values are set equal to the number of input matrices. Following Ohm's Law and Kirchhoff's Circuit Laws, each input is divided by the total number of inputs and then summed, leading to a negative global average current. This negative global average current is converted into a positive global average voltage by TIAs, which serves as the output result.

F. Memristor-Based Fully Connected Module

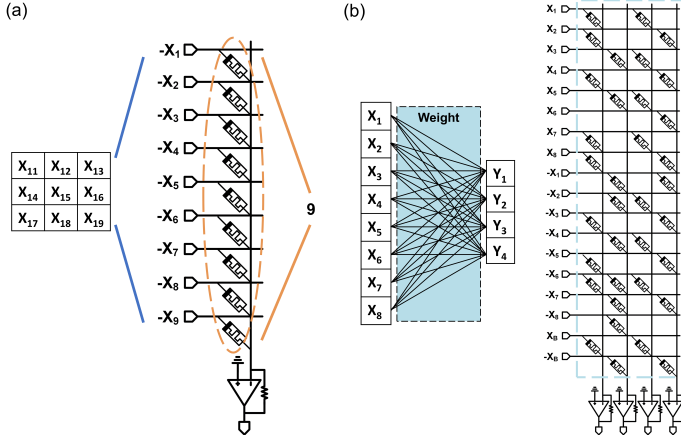


Fig. 5. Circuit schematic of memristor crossbars for (a) a global average pooling operation, (b) a fully connected operation.

The memristor-based fully connected module integrates and normalizes the highly abstracted features after multiple convolutions and outputs a probability for each category of the recognition network. The circuit of the memristor-based fully connected module is similar to that of the memristor-based convolution module, but the size is generally larger and contains more memristors. Compared to convolution modules, it only requires converting the original weight matrix into positive and negative weight matrices, and then arranging them in a vertical sequence.

III. EXPERIMENTS

In this section, we implement the scaled-down MobileNetV3 neural network for a classification application using the CIFAR-10 dataset. Following neural network computation, the CIFAR-10 dataset is categorized into ten distinct labels. The classification result of the memristor-based neural network is determined by identifying the output with the highest current, as verified through SPICE. The network weights are obtained from an offline server that was trained on the CIFAR-10 dataset. Table 1 compares the performance of our study with other neural networks utilizing novel computing paradigms. Our memristor-based MobileNetV3 neural network achieves a high classification accuracy of 90.36% on the CIFAR-10 dataset, exhibiting an improvement over previous works in this area.

TABLE I
PERFORMANCE COMPARISON WITH OTHER NEW COMPUTING PARADIGMS

Publication/Year	Device	Signal	Accuracy(CIFAR-10)
DATE'18 [14]	RRAM	Digital	86.08%
TNSE'19 [12]	memristor	Analog	67.21%
TNNLS'20 [15]	memristor	Analog	84.38%
ISSCC'21 [16]	eDRAM	Analog	80.1%
TCASII'23 [17]	RRAM	Digital	86.2%
TCASII'23 [18]	memristor	Analog	87.5%
This work	memristor	Analog	90.36%

We refer to methods previously reported in the papers to analyze the latency and energy consumption of memristor-based neural networks [12], [15], [19], [20], to determine the latency of our proposed computing paradigm. The response time can be as quick as 100 ps [15]. Therefore, the latency of this circuit can be as low as 1.24 μ s. This is significantly faster than the traditional GPU approach, which has a latency of 165.4 μ s on a server equipped with an RTX 4090. Figure 6 illustrates the distribution of memristor weights across different layers. As observed in Figure 6, the weights of the memristor crossbars predominantly range between -0.2 and 0.2. The power consumption of the memristor-based neural network is derived from the weights of the memristors. Since we have mapped the input data to ± 2.5 mV, we can estimate the maximum predicted power consumption of a single memristor by assuming that all input data is at 2.5 mV and all weights are 0.2. Therefore, the maximum power consumption of memristors can be estimated at 1.1 μ W, and the power consumption of the CMOS circuit required to achieve the same calculation is close to 60 μ W [21].

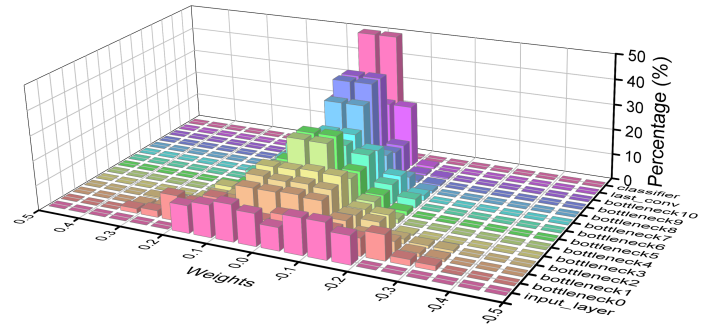


Fig. 6. Distribution of weights of memristors .

IV. CONCLUSION

The memristor-based MobileNetV3 circuit design proposed in this paper demonstrates exceptional performance in accuracy, latency, and energy efficiency for image classification tasks on edge devices. Our optimized memristive modules leverage the advantages of memristors to achieve over 90% accuracy on the CIFAR-10 dataset while significantly reducing inference time and power consumption compared to traditional implementations.

REFERENCES

- [1] S. Woźniak, A. Pantazi, T. Bohnstingl, and E. Eleftheriou, "Deep learning incorporating biologically inspired neural dynamics and in-memory computing," *Nature Machine Intelligence*, vol. 2, no. 6, pp. 325–336, 2020.
- [2] A. Howard, M. Sandler, G. Chu, L.-C. Chen, B. Chen, M. Tan, W. Wang, Y. Zhu, R. Pang, V. Vasudevan, *et al.*, "Searching for mobilenetv3," in *Proceedings of the IEEE/CVF international conference on computer vision*, pp. 1314–1324, 2019.
- [3] K. He, X. Zhang, S. Ren, and J. Sun, "Deep residual learning for image recognition," in *Proceedings of the IEEE conference on computer vision and pattern recognition*, pp. 770–778, 2016.
- [4] C. Li, M. Hu, Y. Li, H. Jiang, N. Ge, E. Montgomery, J. Zhang, W. Song, N. Dávila, C. E. Graves, *et al.*, "Analogue signal and image processing with large memristor crossbars," *Nature electronics*, vol. 1, no. 1, pp. 52–59, 2018.
- [5] O. Mutlu, S. Ghose, J. Gómez-Luna, and R. Ausavarungnirun, "A modern primer on processing in memory," in *Emerging Computing: From Devices to Systems: Looking Beyond Moore and Von Neumann*, pp. 171–243, Springer, 2022.
- [6] R. Chen, W. Zeng, W. Fan, F. Lai, Y. Chen, X. Lin, L. Tang, W. Ouyang, Z. Liu, and X. Luo, "Automatic recognition of ocular surface diseases on smartphone images using densely connected convolutional networks," in *2021 43rd Annual International Conference of the IEEE Engineering in Medicine & Biology Society (EMBC)*, pp. 2786–2789, IEEE, 2021.
- [7] F. Chollet, "Xception: Deep learning with depthwise separable convolutions," in *Proceedings of the IEEE conference on computer vision and pattern recognition*, pp. 1251–1258, 2017.
- [8] B.-S. Hua, M.-K. Tran, and S.-K. Yeung, "Pointwise convolutional neural networks," in *Proceedings of the IEEE conference on computer vision and pattern recognition*, pp. 984–993, 2018.
- [9] B. Li and G. Shi, "A native spice implementation of memristor models for simulation of neuromorphic analog signal processing circuits," *ACM Transactions on Design Automation of Electronic Systems (TODAES)*, vol. 27, no. 1, pp. 1–24, 2021.
- [10] C. Yakopcic, M. Z. Alom, and T. M. Taha, "Memristor crossbar deep network implementation based on a convolutional neural network," in *2016 International joint conference on neural networks (IJCNN)*, pp. 963–970, IEEE, 2016.
- [11] C. Yakopcic, M. Z. Alom, and T. M. Taha, "Extremely parallel memristor crossbar architecture for convolutional neural network implementation," in *2017 International Joint Conference on Neural Networks (IJCNN)*, pp. 1696–1703, IEEE, 2017.
- [12] S. Wen, H. Wei, Z. Yan, Z. Guo, Y. Yang, T. Huang, and Y. Chen, "Memristor-based design of sparse compact convolutional neural network," *IEEE Transactions on Network Science and Engineering*, vol. 7, no. 3, pp. 1431–1440, 2019.
- [13] P. Priyanka, G. Nisarga, and S. Raghuram, "Cmos implementations of rectified linear activation function," in *VLSI Design and Test: 22nd International Symposium, VDAT 2018, Madurai, India, June 28-30, 2018, Revised Selected Papers 22*, pp. 121–129, Springer, 2019.
- [14] X. Sun, S. Yin, X. Peng, R. Liu, J.-s. Seo, and S. Yu, "Xnor-rram: A scalable and parallel resistive synaptic architecture for binary neural networks," in *2018 Design, Automation & Test in Europe Conference & Exhibition (DATE)*, pp. 1423–1428, IEEE, 2018.
- [15] H. Ran, S. Wen, S. Wang, Y. Cao, P. Zhou, and T. Huang, "Memristor-based edge computing of shufflenetv2 for image classification," *IEEE Transactions on Computer-Aided Design of Integrated Circuits and Systems*, vol. 40, no. 8, pp. 1701–1710, 2020.
- [16] S. Xie, C. Ni, A. Sayal, P. Jain, F. Hamzaoglu, and J. P. Kulkarni, "16.2 edram-cim: Compute-in-memory design with reconfigurable embedded-dynamic-memory array realizing adaptive data converters and charge-domain computing," in *2021 IEEE International Solid-State Circuits Conference (ISSCC)*, vol. 64, pp. 248–250, IEEE, 2021.
- [17] Y. Li, J. Chen, L. Wang, W. Zhang, Z. Guo, J. Wang, Y. Han, Z. Li, F. Wang, C. Dou, *et al.*, "An adc-less rram-based computing-in-memory macro with binary cnn for efficient edge ai," *IEEE Transactions on Circuits and Systems II: Express Briefs*, 2023.
- [18] H. Xiao, X. Hu, T. Gao, Y. Zhou, S. Duan, and Y. Chen, "Efficient low-bit neural network with memristor-based reconfigurable circuits," *IEEE Transactions on Circuits and Systems II: Express Briefs*, 2023.
- [19] C. Yang, X. Wang, and Z. Zeng, "Full-circuit implementation of transformer network based on memristor," *IEEE Transactions on Circuits and Systems I: Regular Papers*, vol. 69, no. 4, pp. 1395–1407, 2022.
- [20] W. Zhang, P. Yao, B. Gao, Q. Liu, D. Wu, Q. Zhang, Y. Li, Q. Qin, J. Li, Z. Zhu, *et al.*, "Edge learning using a fully integrated neuro-inspired memristor chip," *Science*, vol. 381, no. 6663, pp. 1205–1211, 2023.
- [21] S. Kim, B. Choi, M. Lim, J. Yoon, J. Lee, H.-D. Kim, and S.-J. Choi, "Pattern recognition using carbon nanotube synaptic transistors with an adjustable weight update protocol," *ACS nano*, vol. 11, no. 3, pp. 2814–2822, 2017.